Clinical Radiology 69 (2014) e223–e229

Contents lists available at ScienceDirect

Clinical Radiology

journal homepage: www.clinicalradiologyonline.net

Pictorial Review

2D and 3D MRI features of classic bladder exstrophy

A. Tekes [a,*], G. Ertan [a], M. Solaiyappan [b], A.A. Stec [c], P.D. Sponseller [d], T.A. Huisman [a], J.P. Gearhart [e]

[a] *Division of Pediatric Radiology, Baltimore, MD, USA*
[b] *Department of Radiology, Russell H. Morgan Department of Radiology and Radiological Science, Baltimore, MD, USA*
[c] *Department of Urology, Medical University of South Carolina, Charleston, SC, USA*
[d] *Department of Orthopaedic Surgery, Baltimore, MD, USA*
[e] *Division of Pediatric Urology, Department of Urology, The Brady Urological Institute, The Johns Hopkins Medical Institutions, Baltimore, MD, USA*

ARTICLE INFORMATION

Article history:
Received 11 October 2013
Received in revised form
9 December 2013
Accepted 18 December 2013

The bladder exstrophy–epispadias complex (EEC) represents a spectrum of rare and surgically correctable congenital anomalies. Classic bladder exstrophy (CBE) stands between epispadias and cloacal exstrophy (CE) in the severity spectrum, and is the most commonly encountered type. CBE involves congenital defects of the bladder, abdominal wall, pelvic floor, and bony pelvis. With the growing understanding of the detrimental effects of radiation in children, magnetic resonance imaging (MRI) is progressively been utilized in the preoperative work-up and post-surgical follow-up of these patients. MRI provides valuable information for planning and evaluating the optimal surgical techniques for closure of CBE. The aim of this paper is to provide a review of the two- (2D) and three-dimensional (3D) MRI features of CBE including a detailed analytical description of the anatomy of the pelvic floor in affected patients.

Introduction

The bladder exstrophy–epispadias complex (EEC) represents a spectrum of rare and surgically correctable congenital anomalies; epispadias being the mildest and cloacal exstrophy being the most severe form. Classic bladder exstrophy (CBE) is the most common variant, and falls in the middle of these categories. (Fig 1) CBE typically presents with congenital defects of the bladder, abdominal wall, pelvic floor, and bony pelvis.

CBE is reported to occur in 1:10,000 to 1:50,000 live births,[1] and is more commonly encountered in boys than in girls, with a reported ratio of between 2.3–6:1.[2,3] The EEC results from a failure of mesenchymal cells to migrate appropriately between the ectoderm of the abdomen and the cloaca, as early as during the fourth week of gestation. Three major hypotheses have been proposed for the embryological origin of EEC: (1) premature rupture of the cloacal membrane,[4] (2) mechanical obstruction of the mesodermal migration,[5] and (3) disruption of cellular function resulting in abnormal development.[6] Although these three aetiological theories may all explain the embryological origin of the EEC independently, the malformation most likely results from a combination of these three assumed aetiologies. Premature rupture of an abnormally formed cloacal membrane attributable to cellular or mechanical causes results in the formation of the exstrophy.

* Guarantor and correspondent: A. Tekes, Division of Pediatric Radiology, Department of Radiology and Radiological Science, Johns Hopkins Hospital, 1800 Orleans Street, Zayed Tower, 4th Floor, Room 4174, Baltimore, MD 21287-0842, USA. Tel.: +1 410 955 6141; fax: +1 410 502 3633.
E-mail address: atekes1@jhmi.edu (A. Tekes).

0009-9260/$ – see front matter © 2014 The Royal College of Radiologists. Published by Elsevier Ltd. All rights reserved.
http://dx.doi.org/10.1016/j.crad.2013.12.019

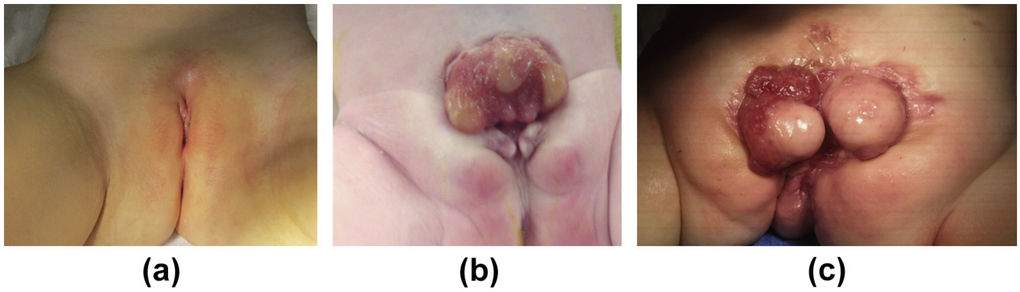

Figure 1 Epispadias (a), classic bladder exstrophy (b), and cloacal exstrophy (c) in three female patients.

The severity of the EEC depends on the timing of the cloacal membrane rupture in relation to the fusion of the urorectal septum to the cloacal membrane. At the completion of embryological development, in addition to the exstrophic urethra, bladder, and/or bowel, the EEC is also accompanied by a complex malformation of the bony pelvis and pelvic floor, which requires surgical correction.[7] Surgical corrections of CBE serves two goals, first closure of the bladder plate to provide a functional urinary reservoir with urinary continence, and second a pleasing and functional cosmesis of the genitalia. Modern staged reconstruction of exstrophy (MRSE) aims to close the bladder, posterior urethra, and abdominal wall with or without osteotomy just after birth followed by a repair of the epispadias at 6 months to 1 year of age, followed by bladder neck reconstruction at 4–5 years of age.[8]

Magnetic resonance imaging (MRI) allows collection of high-resolution, high contrast-to-noise ratio, two- (2D) and three-dimensional (3D) imaging data sets of the pelvis. Moreover, MRI does not use ionizing radiation and is consequently exquisitely well suited to study children with CBE. The 3D acquisition provides important qualitative and quantitative data.[9]

The aim of this paper is to review the normal and abnormal 3D MRI anatomy of the pediatric pelvic floor in children with CBE, before and after surgery. A correct understanding of the normal and abnormal anatomy may guide and provide valuable insight for choosing the optimal surgical technique for closing CBE.

Pelvic floor anatomy

The Belgian anatomist Andreas Vesalius was one of the first to study and publish details about the anatomy of the human pelvic floor. His work dates back to 1555.[10] Many years later, Dickinson referred to the challenge of the proper understanding of the pelvic floor musculature in his publication in 1889 as follows: “There is no considerable muscle in the body whose form and function is more difficult to understand than of the levator ani (LA), and about which such nebulous impressions prevail”.[11] In the new era of advances in histopathological evaluation and radiological imaging, this challenge still remains.

The major muscle that forms the pelvic floor muscle is the LA that is composed of striated muscles fibres. The LA arises anteriorly from the posterior surface of the superior ramus of the pubis, lateral to the symphysis; posteriorly from the inner surface of the spine of the ischium; and between these two points from the obturator fascia.[12] The obturator internus (OI) muscle serves as a frame for the attachment of the LA to the pelvic bones.[13,14] The major components of the LA are a laterally localized thin sheet of muscle called the iliococcygeus (IC) muscle, a bulkier medial muscular sling called the pubococcygeus (PC) muscle, and the puborectalis (PR) muscle. The IC muscle attaches anteriorly to the pubic bone, arcus tendineus of the LA muscle, and posteriorly to the anococcygeal raphe and coccyx. The more substantial part of the LA is the PC muscle, which inserts bilaterally at the pubic rami and wraps around the midline structures of the bladder, urethra, vagina, and rectum. The PC muscle is funnel-shaped with a transverse portion called the LA plate and a vertical portion called the suspensory sling.[14] At the level of the levator hiatus, the plate bends sharply downward to form the suspensory sling. This most medial portion of the LA is the PR sling, which attaches to the midline viscera during passage through the pelvic floor. This muscle provides direct and indirect support for the vagina, bladder, and urethra by pulling these structures ventrally toward the pubic bone.[14,15] In extensive new human anatomy dissections with microscopic confirmation, Shafik et al.[14,15] reported that the PR sling extension of the LA connects to the urethra at the bladder neck.

The various components of the LA have been interpreted differently in the literature resulting in confusion in the nomenclature. In this article, we follow the *Nomina Anatomica* terminology.[16] According to *Nomina Anatomica*,[16] the LA consists of four components: the PC, pubovaginalis (or levator prostate), PR, and IC portion. Of these four components, the PC, PR, and IC can be identified on pelvic MRI studies of young children with normal anatomy and CBE.

Anatomical evaluation of the LA has been widely obtained from dissections or routine anatomopathological preparations of the adult pelvis. Fritsch and Frohlich[17] were the leading researchers to study the LA in foetuses. Anatomopathological evaluation of the LA by Fritsch and Frohlich demonstrated that the LA muscle can be recognized with three distinct portions (PR, PC, IC) as early as the 9th gestational week. Close to the end of the second trimester, the typical funnel shape of the LA forms.[17] The overall shape of the LA is highly dependent on the development of the bony pelvis as previously documented in the computed tomography (CT) evaluation of the pelvis in CBE. In 1995, Sponseller et al.,[18] compared CBE children with age-matched controls, and demonstrated that there is an external rotation of the posterior aspect of the pelvis, typically about 12° on each side. In addition, there is a net external rotation of the anterior pelvis by about 18°, combined with a retroversion of the acetabulum and 30% shortening of the pubic rami in addition to the pubic diastasis.[18]

In 2001, Stec et al.[19,20] demonstrated that external rotation of the pelvis was mostly due to the fact that the sacroiliac joints are 10° more toward the coronal plane than the sagittal. Stec et al.[19,20] also noted that there is a 15° inferior rotation of the pelvis and that the sacrum in exstrophy patients was 43% larger by volume and 24% larger in surface area than in normal controls.

The pelvic bones in children with CBE appear like a more open book or square shape compared to that of controls. Pubic diastasis is typically accompanied by short pubic rami, which may result from a lack of stimulus to grow further toward the midline. The anatomy of the pelvic floor is challenging across all age groups, but especially in the neonate. In adults, the pelvic floor muscles are quite thin, but even thinner in the neonate. The presence of fat serves as a natural contrast and enables differentiation between the various LA muscle groups and pelvic organs. Unlike adults and older children, there is a paucity of fat in the neonatal pelvis, limiting anatomical differentiation of the various pelvic structures in MRI. Moreover, air and faeces within the rectum with resultant MRI susceptibility artefacts may obscure image detail, especially limiting evaluation of the PR muscle.

MRI protocol of CBE

Pre- and post-surgical MRI of the pelvis is the standard of care in the surgical management of CBE in our institution (Johns Hopkins Hospital). Patients are examined using a 1.5 T MRI machine (Avanto, Siemens, Erlangen, Germany). The departmental exstrophy pelvic MRI protocol includes axial, coronal, and sagittal T1-weighted (T1W) and T2-weighted (T2W) turbo spin-echo images of the pelvis without fat suppression with 3 mm section thickness. The field of view (FOV) covers the region from the top of kidneys to the bottom of genitalia in craniocaudal extension and from the skin to skin laterally. Total acquisition time is 18–22 min. Children with CBE are examined using MRI in the first few days of life before surgery and up to 1 year of age after the first stage of repair. Therefore, the imaging parameters, in particular the spatial resolution, are adapted for the size and age of the child.

Overall, in CBE the LA is located more posteriorly and externally rotated and flattened, following the box-like shape of the bony pelvis. The anus is anteriorly displaced (Fig 2) and only one-third of the LA muscle is located anteriorly, providing limited support for the pelvic organs. In males with CBE, the urethral meatus is seen on the dorsal

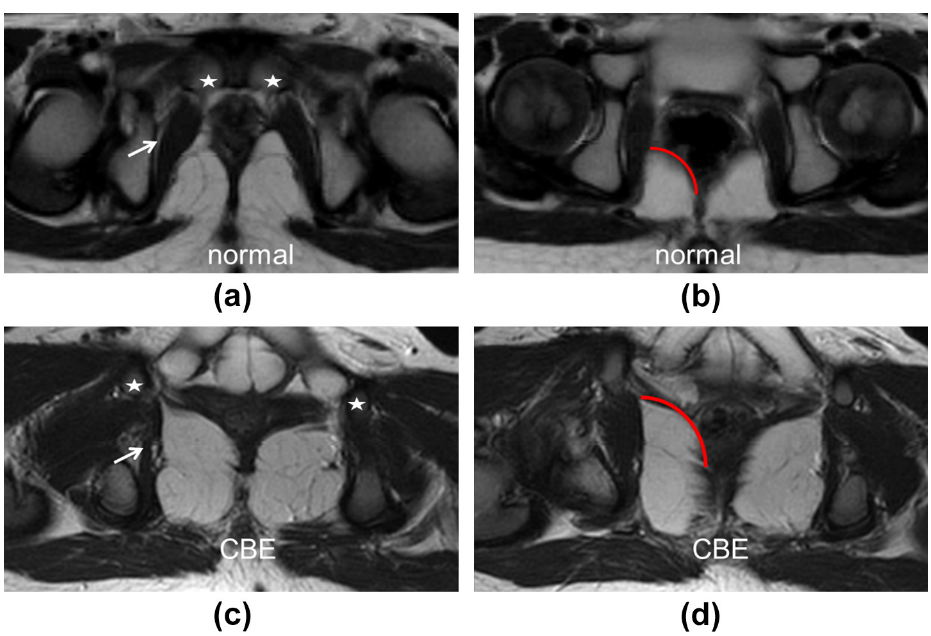

Figure 2 The PR muscle can be best visualized in the axial plane. The course of the PR is drawn in axial T2W images in red at the level of the OI muscle (arrow) in the normal control (b) and CBE (d): the PR is elongated and flattened in CBE. Note the oblique course of the iliacus internus muscle in normal control (arrow) (a) as opposed to vertical orientation in CBE (arrow) (c). The star marks on the medial ends of the pubic bones in normal control (a) and CBE (c) demonstrates the pubic diastasis in (c) with increased distance between the medial ends of the pubic bones. With diastasis of the pubic bones, there is also resultant diastasis of the erectile bodies. Pubic diastasis and pelvic floor flattening result in an open-book configuration of the pelvis in CBE (second row) as opposed to the normal control (first row). (For interpretation of the references to color in this figure legend, the reader is referred to the web version of this article.)

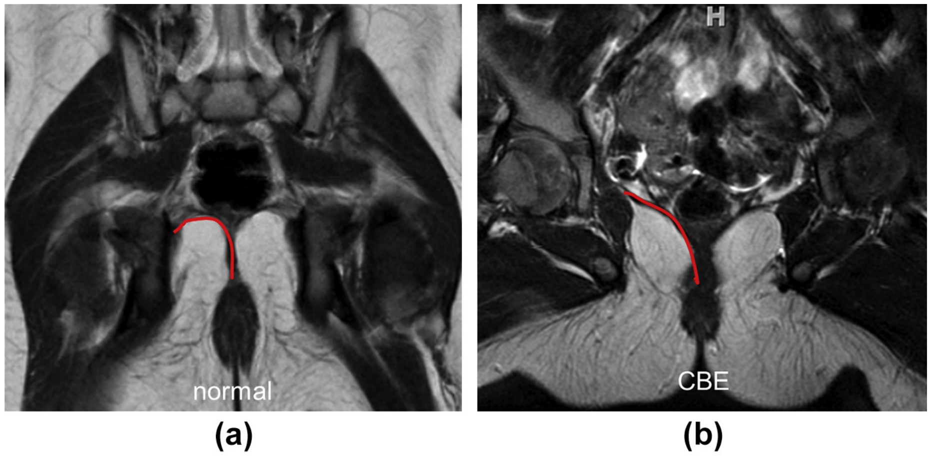

Figure 3 The IC can be best visualized in the coronal plane. The course of the IC is drawn in red at the level of the rectum in the normal control (a) and CBE (b). The IC muscle has the appearance of a Christmas candy cane in the normal control (a), as opposed to a flattened/elongated arc in CBE (b). (For interpretation of the references to color in this figure legend, the reader is referred to the web version of this article.)

aspect of the phallus, which is typically shortened. The corpora cavernosa are splayed due to the pubic diastasis contributing to the short phallus. The umbilicus is low-set and can be associated with umbilical hernias. Indirect inguinal hernias are common.

2D evaluation of the LA can be done on a patient archiving and communication system (PACS). During imaging analysis, the three major muscles of the LA can be distinguished: the PR (Fig 2), IC (Fig 3), and PC (Fig 4). The PR is best visualized in the axial plane (Fig 2). The orientation of the OI muscle is vertical in CBE (Fig 2). Pubic diastasis and external rotation of the sacrum results in a wider distance in the lower pelvis, with an elongated and flattened LA in CBE compared to a normal control. The IC is best demonstrated in the coronal plane (Fig 3), extending along each side of the rectal wall and attaching to the iliacus internus. Normally, the IC muscle has the appearance of a "Christmas candy cane" as opposed to a flattened/elongated

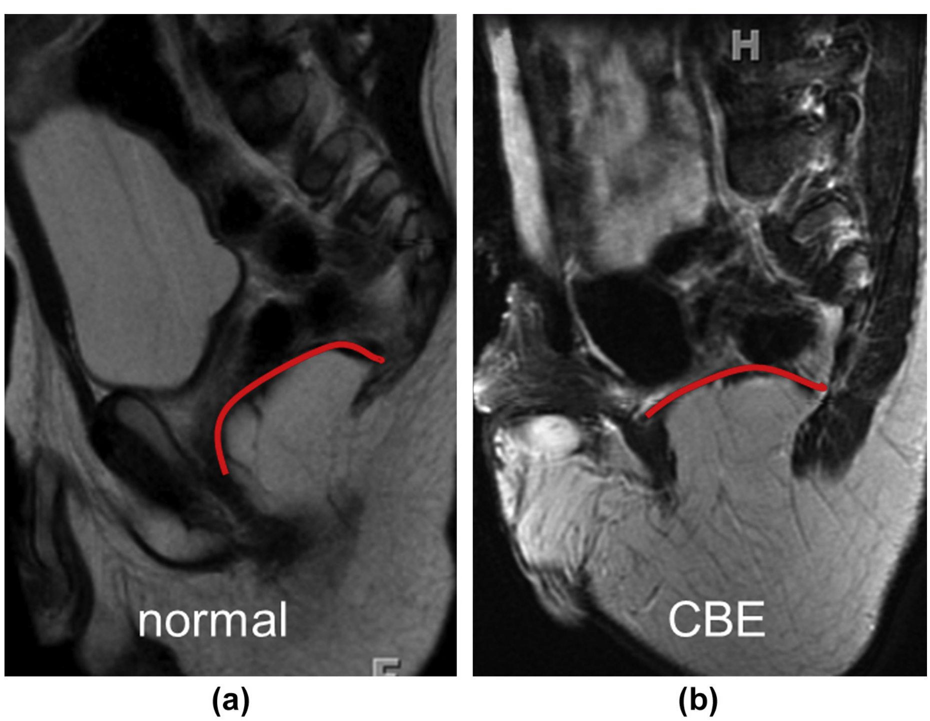

Figure 4 The PC muscle can be best visualized in the sagittal plane. The course of the PC is drawn in sagittal T2W images in red extending between the inner surface of the medial aspect of the pubis and tip of the coccyx in the normal control (a) and CBE (b). Note the flatted curve of the PC muscle in CBE (b) as opposed to the normal control (a). (For interpretation of the references to color in this figure legend, the reader is referred to the web version of this article.)

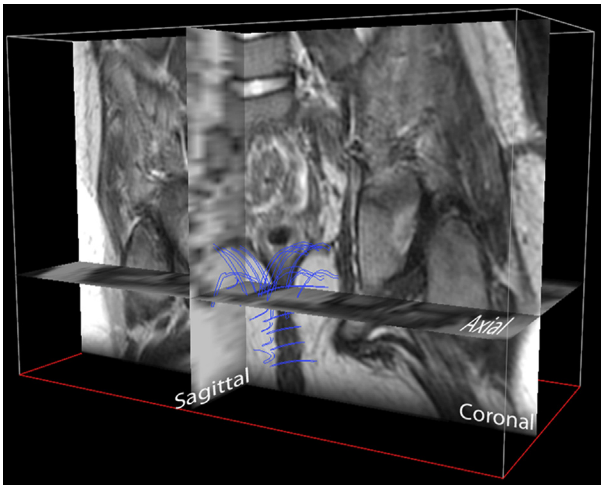

Figure 5 The contours of the PR, IC, and PC are drawn bilaterally on multiple sections as far can the muscle groups can be identified in axial, coronal, and sagittal planes. Then the contour data set is co-registered in all three planes as shown in this figure. Note that the PR (axial) is the lowest and the IC (coronal) makes the highest part of the LA.

arc in CBE patients (Fig 3). The PC is best demonstrated in the sagittal plane close to midline (Fig 4), extending between the inner surface of the medial aspect of the pubis and tip of the coccyx.

3D visualization systems may offer measurements of the entire muscle group rather than a single section of the muscle only. This approach renders a more realistic understanding of the pelvic floor before and after surgery. When the whole muscle group is visualized in a 3D system, orientation/overall curvature of the muscle group can be measured, from which a quantitative and qualitative analysis can be performed. A Dextroscope® is used for 3D stereoscopic evaluation, which provides a natural and intuitive hand–eye coordination to explore the 3D funnel shape of the LA. The US Food and Drug Administration (FDA) approved the Dextroscope in 2001. It is a standalone system integrating hardware and software that connects to the clinical workflow by means of digital imaging and communications in medicine (DICOM) data, either via the PACS or compact disc-read only memory (CDROM). It provides a stereoscopic hand–eye coordinated 3D interface of the medical images. The volumes made of DICOM data can be conveniently visualized with 3D stereoscopic depth perception using two hands, one holding a 3D stylus for intuitive operating (crop, drill, measure) with the volumetric dataset and another holding a joystick to control position and orientation of the patient data.[21] The pelvis MRI data (DICOM images) are transferred from the PACS to this off-line post-processing standalone visualization system. Dextroscope was initially tailored for neurosurgery planning,[22] and has since found use in other specialties such as otolaryngology, cardiovascular interventions, and virtual colonoscopy to name a few.

The contours of each LA muscle group are manually drawn on each side, for every section where the muscle can be identified. The contour data for PR, IC, and PC are subsequently co-registered in each respective plane (Fig 5). Quick qualitative analysis of the pelvic floor can easily be performed in this co-registered contour data set. PR is the lowest, and IC is the highest part of the LA. Contour analysis can be performed either for quantitative or for qualitative analysis. The impact of surgery can be demonstrated before and after surgery for a quick qualitative evaluation of the results (Fig 6). This dedicated approach of drawing the muscle contour enhances the qualitative assessment of the contours: in children with CBE, muscle contour irregularities improve after surgery (Fig 6). After drawing all the muscle contours, an average contour can be obtained from each group and used for quantitative analysis. In addition to qualitative comparisons, quantitative measurements can be performed (Fig 7). Chord measurements allow quantification and standardization of the degree of curvature of an arc, specifically defined as the mean ratio of the arc length over the chord length of a curved contour. We prefer chord measurements over absolute length measurements, because by taking the ratio of the curvature of the arc over the length of the arch, one can take into account the growth of the child. This enables comparisons between different age groups in a more reliable fashion, such as in the setting of pre and post-surgical evaluation. Chord measurements can be performed in each part of the LA: PR, IC, and PC.

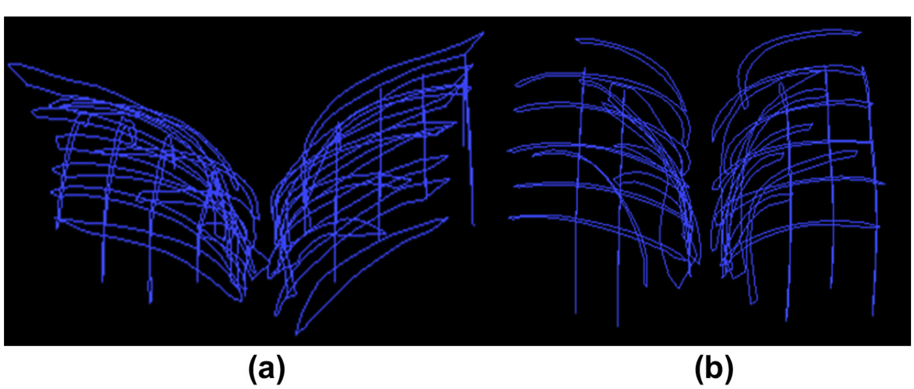

Figure 6 Qualitative evaluation of the pelvic floor with the 3D data set: comparison of preoperative (a) and postoperative (b) contours of the LA. After closure, all three muscle groups of the LA appear deeper in CBE (b), providing a more conical shape. In addition, note the irregularities in the contour of the muscle groups (a) that improve after surgical intervention (b).

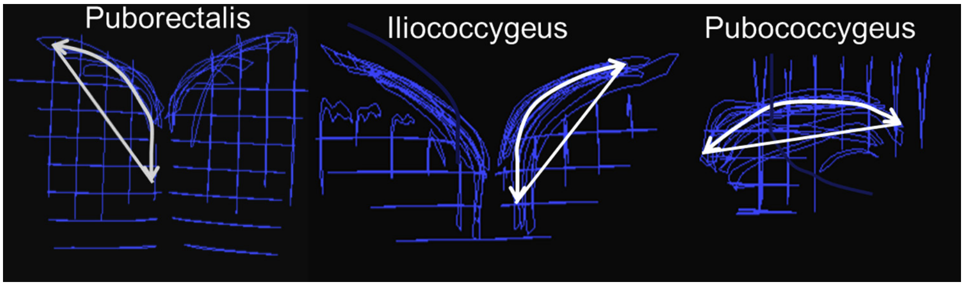

Figure 7 Quantitative evaluation of the pelvic floor with the 3D data set. Once the contour data set is created, geometric analysis of the contours can be done to evaluate the LA. The contours of each muscle are drawn in multiple sections (blue); therefore, the mean of the curvature is calculated for each muscle group (white). Then the ratio of the arc length over the chord length is calculated. The advantage of this method is twofold: (1) the contours of each muscle group are drawn in multiple sections; therefore, each section of the muscle group is taken into consideration rather than a single representative section, and (2) by dividing the cord length over the arc length, one can factor in the impact of growth of the child. (For interpretation of the references to color in this figure legend, the reader is referred to the web version of this article.)

Conclusion

CBE is a rare congenital anomaly that requires careful evaluation of the pelvic floor for optimal surgical outcome. Pelvic floor muscles form a thin layer of muscle providing major support and optimal function for the urogenital and reproductive systems. Such challenging and complex anatomy becomes even more challenging in the small-sized neonatal pelvis with very little pelvic fat.

The normal conical shape of the pelvis is highly affected by the bony pelvis; therefore, pelvic osteotomies can provide additional value to primary bladder closure. Growing evidence and awareness of the detrimental effects of radiation especially on the growing child make MRI the imaging technique of choice for the diagnostic work-up of the paediatric pelvic floor. In addition, the high soft-tissue resolution and excellent spatial resolution are of benefit.[23–25]

Traditionally angle, length, and thickness measurements have been done of the LA for the evaluation of the pelvic floor. This type of evaluation can be done on a PACS workstation. 2D analysis of the pelvic floor and bony pelvis using CT and MRI have been previously described.[19–25] However, when one needs to make comparisons between a newborn pelvic MRI obtained in the first few days of life, compared to a follow-up examination at 6 months or later, length and thickness measurement comparisons can be unreliable. 3D post-processing tools may compensate for this and give important follow up data.

Long-term, our technique may allow for detailed dissection of the postoperative changes as they relate to functional outcomes, such as continence, which is critical for the quality of life in children CBE. In summary, combined high-end 2D and 3D MRI is the technique of choice for the evaluation of paediatric pelvic floor in the pre-surgical planning, and for the postoperative evaluation of the various surgical approaches applied for repair of CBE.

References

1. Lattimer JK, Smith MJ. Exstrophy closure: a followup on 70 cases. *J Urol* 1966;**95**:356–9.
2. Epidemiology of bladder exstrophy and epispadias: a communication from the International Clearinghouse for Birth Defects Monitoring Systems. *Teratology* 1987;**36**:221–7.
3. Shapiro E, Lepor H, Jeffs RD. The inheritance of the exstrophyepispadias complex. *J Urol* 1984;**132**:308–10.
4. Muecke EC. The role of the cloacal membrane in exstrophy: the first successful experimental study. *J Urol* 1964;**92**:659–67.
5. Manner J, Kluth D. The morphogenesis of the exstrophy–epispadias complex: a new concept based on observations made in early embryonic cases of cloacal exstrophy. *Anat Embryol (Berl)* 2005;**210**:51–7.
6. Cheng W, Jacobs WB, Zhang JJ, et al. DeltaNp63 plays an anti-apoptotic role in ventral bladder development. *Development* 2006;**133**:4783–92.
7. Stec AA. Embryology and bony and pelvic floor anatomy in the bladder exstrophy–epispadias complex. *Semin Pediatr Surg* 2011;**20**:66–70.
8. Gearhart JP. Complete repair of bladder exstrophy in the newborn: complications and management. *J Urol* 2001;**165**:2431–3.
9. Stec AA, Tekes A, Ertan G, et al. Evaluation of pelvic floor muscular redistribution after primary closure of classic bladder exstrophy by 3-dimensional magnetic resonance imaging. *J Urol* 2012;**188**(Suppl.):1535–42.
10. Gabriel WB. *The principles and practice of rectal surgery*. 5th ed. London: Lewis & Co.; 1963.
11. Dickinson R. Studies of levator ani muscle. *Am J Obstet* 1889;**9**:898–917.
12. Yavagal S, de Farias TF, Medina CA, et al. Normal vulvovaginal, perineal, and pelvic anatomy with reconstructive considerations. *Semin Plast Surg* 2011;**25**:121–9.
13. Strohbehn K. Normal pelvic floor anatomy. *Obstet Gynecol Clin North Am* 1998;**25**:683.
14. Shafik A. Levator ani muscle: new physioanatomical aspects and role in the micturition mechanism. *World J Urol* 1999;**17**:266–73.
15. Shafik A. A new concept of the anatomy of the anal sphincter mechanism and the physiology of defecation. VIII. Levator hiatus and tunnel: anatomy and function. *Dis Colon Rectum* 1979;**22**:539–49.
16. Warwick R. *Nomina Anatomica*. 5th ed. London: William & Wilkins; 1983.
17. Fritsch H, Frohlich B. Development of the levator ani muscle in human fetuses. *Early Hum Dev* 1994;**37**:15–25.
18. Sponseller PD, Bisson LJ, Gearhart JP, et al. The anatomy of the pelvis in the exstrophy complex. *J Bone Joint Surg Am* 1995;**77**:177–89.
19. Stec AA, Pannu HK, Tadros YE, et al. Pelvic floor anatomy in classic bladder exstrophy using 3-dimensional computerized tomography: initial insights. *J Urol* 2001;**166**:1444–9.
20. Stec AA, Pannu HK, Tadros YE, et al. Evaluation of the bony pelvis in classic bladder exstrophy by using 3D-CT: further insights. *Urology* 2001;**58**:1030–5.
21. Poston T, Serra L. Dextrous virtual work. *Communications of the ACM* 1996;**39**:37–45.
22. Kockro RA, Serra L, Tseng-Tsai Y, et al. Planning and simulation of neurosurgery in a virtual reality environment. *Neurosurgery* 2000;**46**:118–35. discussion 135–7.

23. Halachmi S, Farhat W, Konen O, et al. Pelvic floor magnetic resonance imaging after neonatal single stage reconstruction in male patients with classic bladder exstrophy. *J Urol* 2003;**170**:1505–9.
24. Williams AM, Solaiyappan M, Pannu HK, et al. 3-Dimensional magnetic resonance imaging modeling of the pelvic floor musculature in classic bladder exstrophy before pelvic osteotomy. *J Urol* 2004;**172**:1702–5.
25. Gargollo PC, Borer JG, Retik AB, et al. Magnetic resonance imaging of pelvic musculoskeletal and genitourinary anatomy in patients before and after complete primary repair of bladder exstrophy. *J Urol* 2005;**174**:1559–66. discussion 1566.